

## Kramers – Kronig's Analysis of $\text{Hg}_{1-x}\text{Fe}_x\text{S}$ Cubic Crystals

DR. Ammar Sarem\*

(Received 12 / 6 / 2007. Accepted 8/11/2007)

### □ ABSTRACT □

The results of Kramers- Kronig analysis of all the reflectivity spectra were reported based on the results of interband optical transitions observed by means of reflectivity measurements of  $\text{Hg}_{1-x}\text{Fe}_x\text{S}$  ( $x=0.01, 0.04$  and  $0.06$ ) crystals in the energy range  $1.5\text{--}12\text{eV}$ . We used a computer program for Kramers-Kronig analysis to determine the  $\epsilon_{\text{Re}}$  and  $\epsilon_{\text{Im}}$  spectra. The observed dependence of the positions of the spectral peaks on the Fe content allows us to estimate the contribution of Fe-derived states to the band structure of  $\beta\text{-HgS}$  semiconductor. The interpretation of structures spectra as a result of interband transitions between occupied valence bands and the empty conduction bands are presented along with some conclusions concerning the electronic band structure of  $\beta\text{-HgS}$ .

Kramers-Kronig analyses were carried out at the Department of Physics, Faculty of Science, Tishreen University.

---

\*Professor, Department of Physics, Faculty of Science, Tishreen University, Latakia, Syria.

## تحليل كرامرز-كرونيغ للبلورات المكعبة $Hg_{1-x}Fe_xS$

الدكتور عمّار صارم\*

(تاريخ الإيداع 12 / 6 / 2007. قُبل للنشر في 8/11/2007)

### □ الملخص □

عرضت نتائج تحليل كرامرز-كرونيغ لجميع أطيف الانعكاسية، اعتماداً على نتائج الانتقالات الضوئية ما بين العصابات بواسطة قياسات الانعكاسية للبلورات  $Hg_{1-x}Fe_xS$  ( $x=0.01, 0.04, 0.06$ ) في مجال الطاقة من 1.5 إلى 12 eV. استخدمنا برنامج حاسوبي لتحليل كرامرز-كرونيغ لتحديد الأطيف  $Re$  و  $Im$ . تبين أن علاقة مواقع القمم الطيفية الملاحظة بتركيز الحديد تسمح لنا بتقدير مشاركة سويات الحديد في البنية العصابية لنصف الناقل  $\beta$ -HgS. فسرت بنى الأطيف كنتيجة للانتقالات الداخلية ما بين عصابات التكافؤ المملوءة وعصابات الناقلية الفارغة، وقد أوضحنا استنتاجاتنا الخاصة بالبنية الإلكترونية للبلورة  $\beta$ -HgS.

تم تحليل نتائج كرامرز-كرونيغ في قسم الفيزياء من كلية العلوم بجامعة تشرين.

\* أستاذ في قسم الفيزياء من كلية العلوم بجامعة تشرين، اللاذقية - سورية.

## I. Introduction:

Many of the diluted magnetic semiconductors (DMS) based on II-VI compounds have been thoroughly investigated since the 70s, and their electric, magnetic and optical properties were determined and the electronic band structures of almost those crystals which crystallize in the zinc blend or wurtzite structure are well described [1-5]. Mercury sulphide is an exception among mercury chalcogenides. The cubic modification of  $\beta$ -HgS, is stable at above 550 K, but it transforms upon cooling into  $\alpha$ -HgS [6]. Thus, big size, bulk monocrystals of cubic HgS have not been available to experimentators until quite recently. Some information about crystal structure and electronic properties of  $\beta$ -HgS was obtained from experiments performed for a powder produced by chemical precipitation [1], vacuum-evaporated thin films [1] or a natural polycrystalline material highly doped with Fe [5].

However, a technique of stabilization of the cubic lattice in big monocrystals of HgS grown by means of an equilibrium method has been proposed [7]. It is based on doping the crystals with a transition metal (e.g. Fe, Co or Se). That achievement made it possible to investigate further properties of  $\beta$ -HgS with prospects to compare the results with those known for HgTe and HgSe as well as for the cinnabar form of HgS. Moreover, a new group of solid solutions (DMS) has been obtained. The opportunity arose to fill the gap in the set of data concerning properties of II-VI based diluted magnetic semiconductors.

It has been verified by means of optical and transport measurements that  $\beta$ -HgS is a narrow-gap semiconductor with an inverted band structure [7]. The only attempt to investigate the electronic band structure in the whole Brillouin zone was performed by means of reflectivity studies on good-quality thin evaporated layers [1].

An empirically adjusted first-principle orthogonalized plane wave (OPW) electronic band structure calculation for  $\beta$ -HgS using non-relativistic formalism was carried out by Herman et al [3]. The results were confirmed by calculations by Philips and van Vechten [4]. The only comparison between theoretical [3] and experimental data taken for vacuum evaporated layers of  $\beta$ -HgS was made by Riccius and Siemsen [2]. In the papers mentioned above the agreement between the calculated and experimental energy values of most optical transitions was reasonably good.

To our knowledge there is no Kramers-Kronig analysis study among the reported experiments performed for various forms of cubic  $\beta$ -HgS. The purpose of this paper is to use the reflectivity data, published previously [8], to study their electronic structures, as well as to recognize the regions in the Brillouin zone for which the Fe contribution leads to changes of the electronic structure.

## II. Results and Discussion:

The reflectivity spectra of  $\text{Hg}_{1-x}\text{Fe}_x\text{S}$  crystals (Fig.1) show systematic changes in the positions and shapes of the peaks for samples with different composition. The curves obtained for  $\text{Hg}_{1-x}\text{Fe}_x\text{S}$  compounds were compared with those obtained for HgSe. The electronic band structure and corresponding reflectivity spectra of HgSe crystal are well known from the literature [9]. In the ternary alloys, however, crystalline disorder appears as a result of the local structure (the Hg-S distance is different from the Fe-S distance) as well as chemical disorder, caused by a random distribution of  $\text{S}^{2-}$  anions in the lattice of the  $\text{Hg}_{1-x}\text{Fe}_x\text{S}$  compounds. This can lead to a considerable broadening and some shift of the reflectivity structures and makes their interpretation more complex.

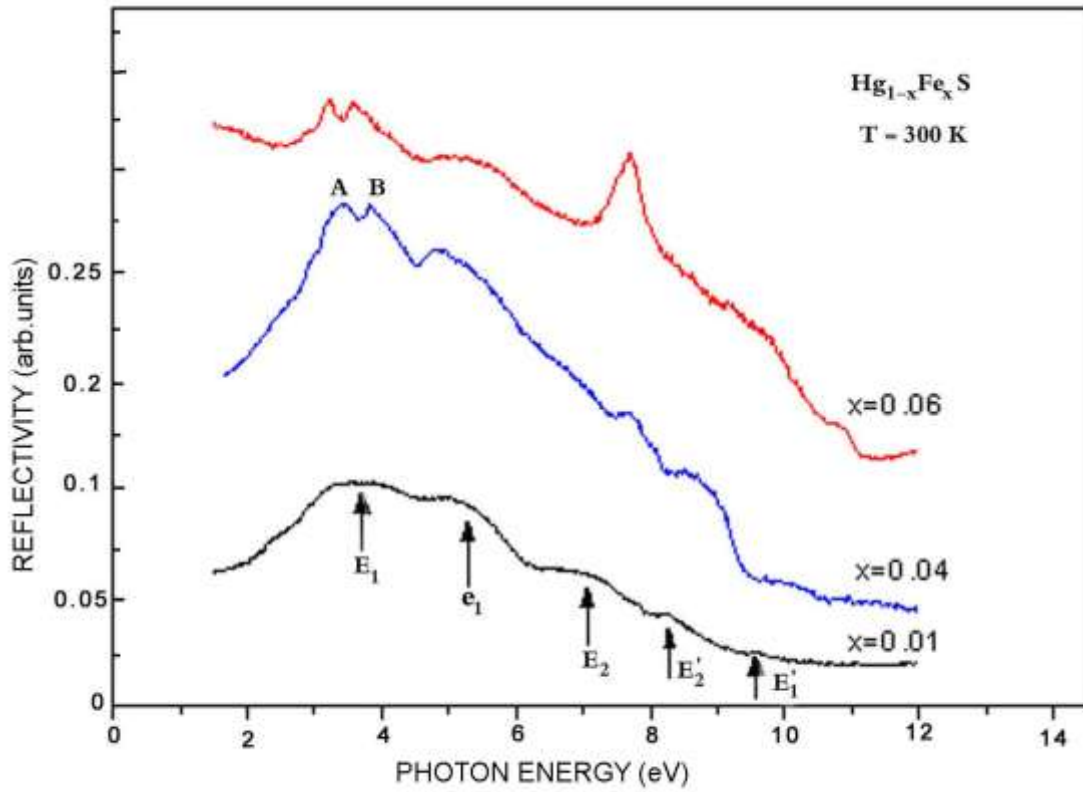


Figure 1. Reflectivity spectra of  $Hg_{1-x}Fe_xS$  crystals at room temperature versus energy [after 8].

All spectra obtained in the experiment were treated using a Kramers - Kronig analysis in order to calculate values for the optical constants  $n$ ,  $k$ ,  $\epsilon_1$  and  $\epsilon_2$ .  $\epsilon_2$  spectra are directly related to the joint density of states distribution.

The complex  $\epsilon(\omega)$  describes a phase shift between two amplitudes. We can write the Kramers - Kronig relations in the form [10, 11]:

$$\epsilon_1(\omega) = 1 + \frac{2}{\pi} P \int_0^{\infty} \frac{\omega_0 \epsilon_2(\omega_0)}{\omega_0^2 - \omega^2} d\omega_0 \quad (1)$$

$$\epsilon_2(\omega) = -\frac{2\omega}{\pi} P \int_0^{\infty} \frac{\epsilon_1(\omega_0)}{\omega_0^2 - \omega^2} d\omega_0 \quad (2)$$

where P means the Cauchy principal value of the integral. Dispersion relations can be given for  $n$  and  $k$  as well as  $Re(1/\epsilon)$  and  $Im(1/\epsilon)$  in a form completely analogous to equations (1) and (2) for  $\epsilon_1$  and  $\epsilon_2$ . As we know, the most useful form of the dispersion relations for the determination of  $n$  and  $k$  from normal incidence reflection data is that which determines the phase angle  $\Theta$ . The complex amplitude reflection coefficient  $r = |r| e^{i\Theta}$  expresses a linear relationship between the amplitudes of reflected and incident light. Therefore there exists a dispersion relation connecting the real and the imaginary parts of

$$\ln r = \ln |r| + i\Theta = \frac{1}{2} \ln R + i\Theta$$

where reflectivity coefficient connects with optical constants as follows:

$$r(\omega) e^{i\Theta(\omega)} = \frac{n(\omega) - 1 + ik(\omega)}{n(\omega) + 1 + ik(\omega)}$$

$$n(\omega) = \frac{1 - r^2(\omega)}{1 + r^2(\omega) - 2r(\omega) \cos \Theta(\omega)}$$

and

$$k(\omega) = \frac{2r(\omega) \sin \Theta(\omega)}{1 + r^2(\omega) - 2r(\omega) \cos \Theta(\omega)}$$

Therefore

$$\varepsilon_1 = n^2 - k^2$$

$$\varepsilon_2 = 2nk$$

The Kramers - Kronig analysis of the reflectivity spectra was based on the following formula [10, 11]:

$$\Theta = \frac{\omega_0}{\pi} \int_0^{\infty} \frac{\ln [R(\omega) / R(\omega_0)]}{\omega_0^2 - \omega^2} d\omega \quad (3)$$

Since  $R(\omega)$  spectra have been taken from 1.5 to 12 eV, the  $R(\omega)$  function had to be extrapolated in order to calculate the integral. In the low energy region, below 1.5 eV, the reflectivity spectra were approximated as  $(a\omega^2 + b\omega + c)$ , where two of the three parameters  $a$ ,  $b$ , and  $c$  were taken to fulfill the continuity of the reflectivity curve and its derivative. Unfortunately, it was impossible to perform direct transmission measurements of the  $Hg_{1-x}Fe_xS$  crystals due to the high value of the free-carrier absorption coefficient. Such measurements allow one to select the appropriate value of the third parameter for approximation of unknown part of integral from equation (3) (for an energy range below 1.5eV). However, this integral, calculated using many different values of the parameter  $a$ , seems to be insensitive to  $a$  value, and the value  $a=0$  was used in calculations.

In the energy region above 12 eV the reflectivity was assumed to be given by:

$$R(\omega) = R_x (\omega_x / \omega)^4 \quad (4)$$

when  $R_x$  and  $\omega_x$  are the reflectivity coefficient and the frequency at the end of the measured spectrum. Equation (3) is applied to an analysis of the reflectivity spectrum, giving the phase angle of reflection as a function of the energy of light. For every point where  $R$  and  $\Theta(\omega)$  are known, other pairs of optical constants can be calculated  $[(n, k)$  and then  $(\varepsilon_1, \varepsilon_2)]$ . The absorption coefficient  $\square$  can be easily obtained from the extinction coefficient  $k$ . A comparison of the calculated and measured values of this constant enables us to check the correctness of the assumed values of the extrapolation parameters. These may be modified until the correspondence is satisfactory.

Figures (2), 3(a), 3(b), 4(a) and 4(b) show the Kramers-Kronig analysis of the reflectivity data. Figure 5 shows the calculation band structure of HgS [12], together with the optical transitions observed in this work.

Since the changes are clearly correlated with an increase of Fe content, they can be regarded as a manifestation of the modifications arising in the band structure of the crystal. The assignments of the spectral features to optical identify the regions in the Brillouin zone where changes in the band structure are most pronounced. This observation will be supported and elaborated in the discussion of the Kramers-Kronig analysis of the spectra.

The main results of the study are displayed in Table I, which shows a comparison between the energy of the peaks and shoulders observed in the  $R(h\nu)$  and  $\varepsilon_2(h\nu)$  curves of the  $\text{Hg}_{1-x}\text{Fe}_x\text{S}$  crystals. The reason for performing the Kramers-Kronig analysis was that  $\varepsilon_2(h\nu)$  spectra describe the optical transitions more directly than the  $R(h\nu)$  itself. However, the features in the reflectivity spectra of the  $\text{Hg}_{1-x}\text{Fe}_x\text{S}$  are more distinct than the corresponding features of  $\varepsilon_2(h\nu)$ . So both the energy positions of the structures and their evolution could be better determined. That makes  $R(h\nu)$  very useful for interpretation of optical transitions of  $\text{Hg}_{1-x}\text{Fe}_x\text{S}$ .

**TABLE I. The energies of the peaks and shoulders discerned in the  $\varepsilon_2(h\nu)$  curves of  $\text{Hg}_{1-x}\text{Fe}_x\text{S}$  crystals obtained by means of a Kramers-Kronig analysis and in the  $R(h\nu)$  curves, together with their assignment to interband transitions.**

Energies ( in eV) of the peaks						
Im $\square\square$ Fe contents			Reflectivity Fe content			Assignment
x=0.01	x=0.04	x=0.06	x=0.01	x=0.04	x=0.06	
3.46	3.38	3.22	3.56	3.48 3.86	3.24 3.56	$E_1 (\Lambda_3^v - \Lambda_1^c)$
4.99	4.63	4.80	5.00	4.97	5.22	$e_1 (L_3^v - L_1^c)$
6.72	7.54	7.44	7.05	7.62	7.70	$E_2 (X_5^v - X_1^c)$
8.20	8.39	8.41	8.25	8.66	9.58	$E_2' (X_3^v - X_1^c)$
9.5	9.92	10.80	9.56	10.04	10.68	$E_1' (L_3^v - L_3^c)$

Since the character of the  $\square\square(h\nu)$  function is directly connected with the joint density of states distribution, the maxima of spectrum  $\square\square(h\nu)$  [shown in Fig. 3(b)] can be ascribed to Van Hove singularities. The energy positions and heights of the peaks correspond to the energies of optical excitations and their strengths, respectively. Thus, the changes in the shapes of the spectra caused by an increase of the Fe content reveal modifications of  $E(\vec{k})$ .

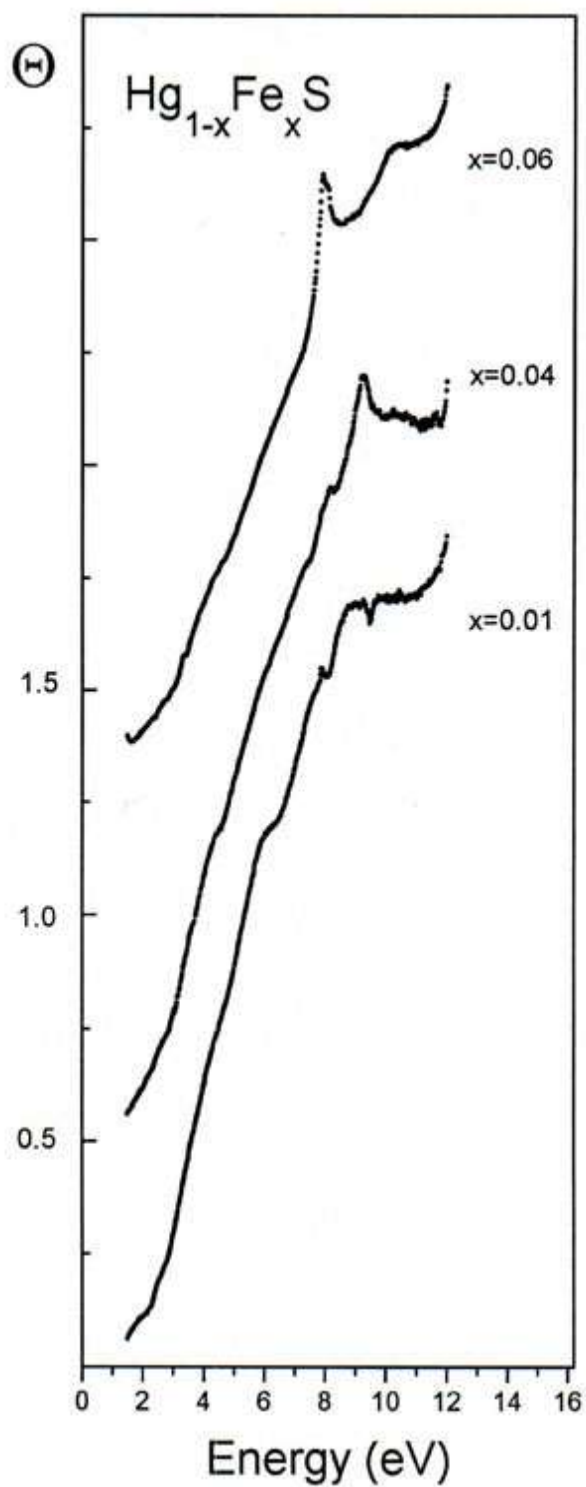


Figure 2. Phase angle  $\Theta$  calculated by the Kramers-Kronig analysis versus energy.

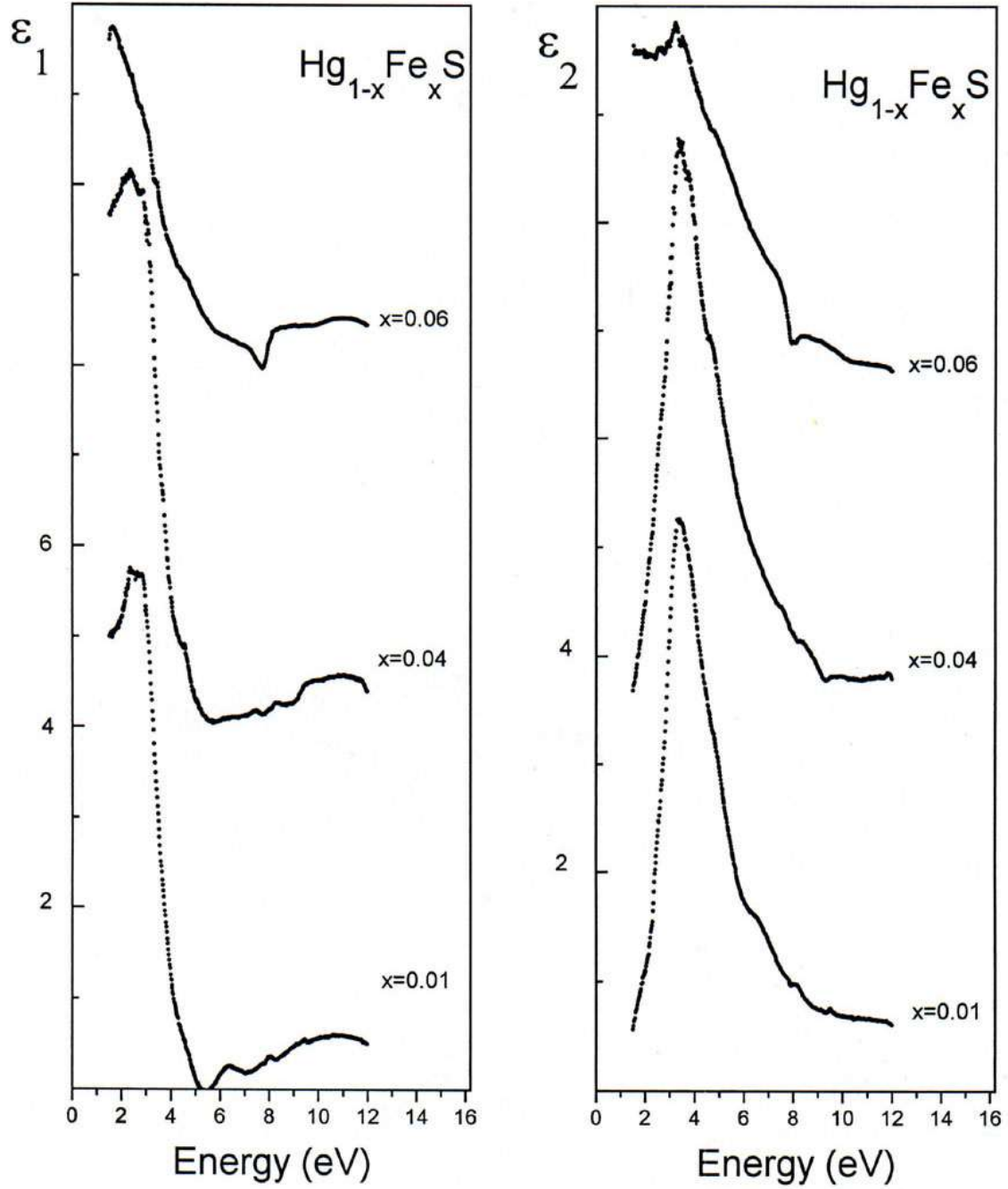


Figure 3. (a) Real part of the dielectric constant  $\epsilon_1$  and (b) imaginary part of the dielectric constant  $\epsilon_2$  of  $\text{Hg}_{1-x}\text{Fe}_x\text{S}$  crystals calculated by the Kramers-Kronig analysis versus energy.

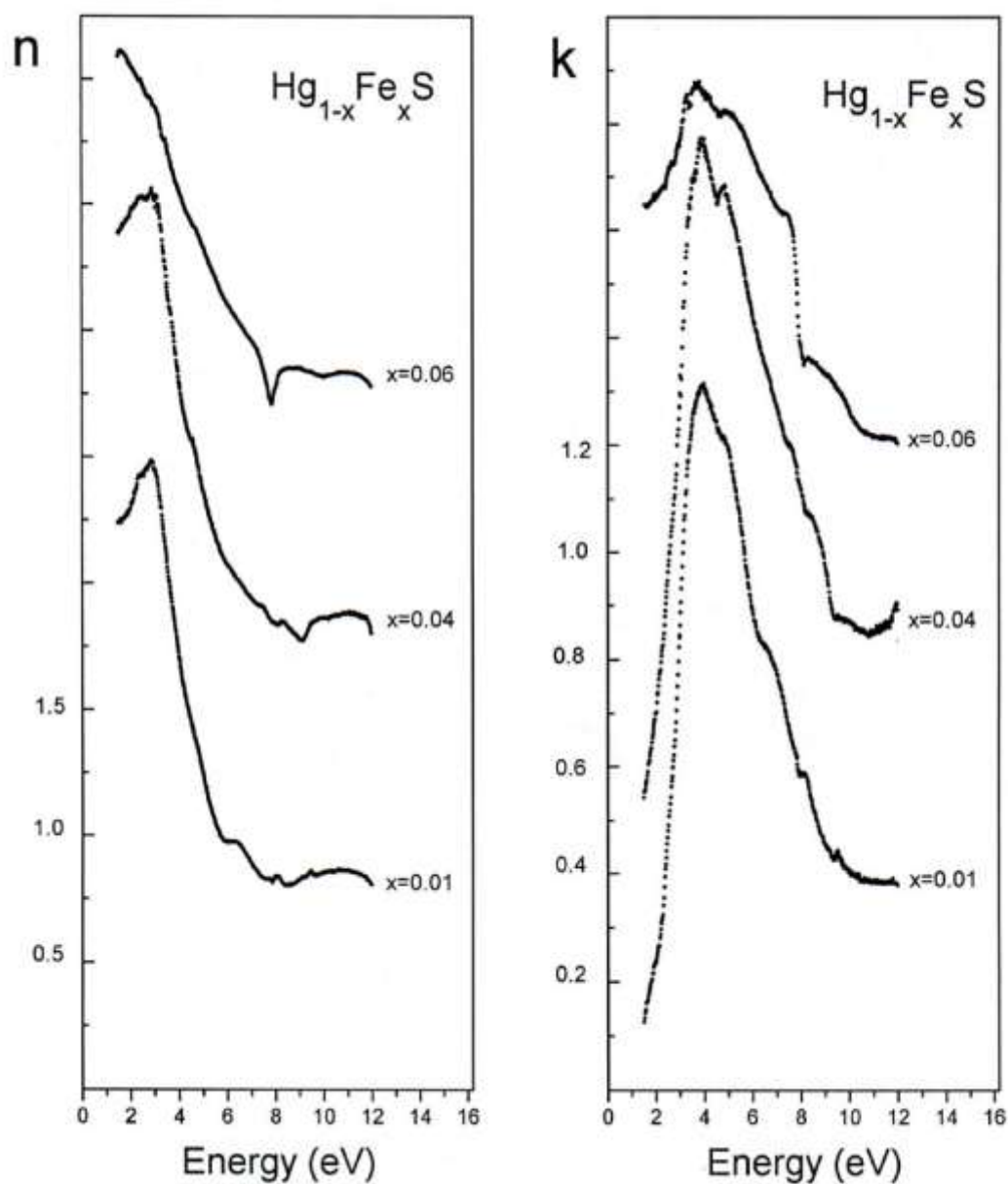


Figure 4. (a) Refraction coefficient  $n$  and (b) extinction coefficient  $k$  of  $\text{Hg}_{1-x}\text{Fe}_x\text{S}$  crystals calculated by the Kramers-Kronig analysis versus energy.

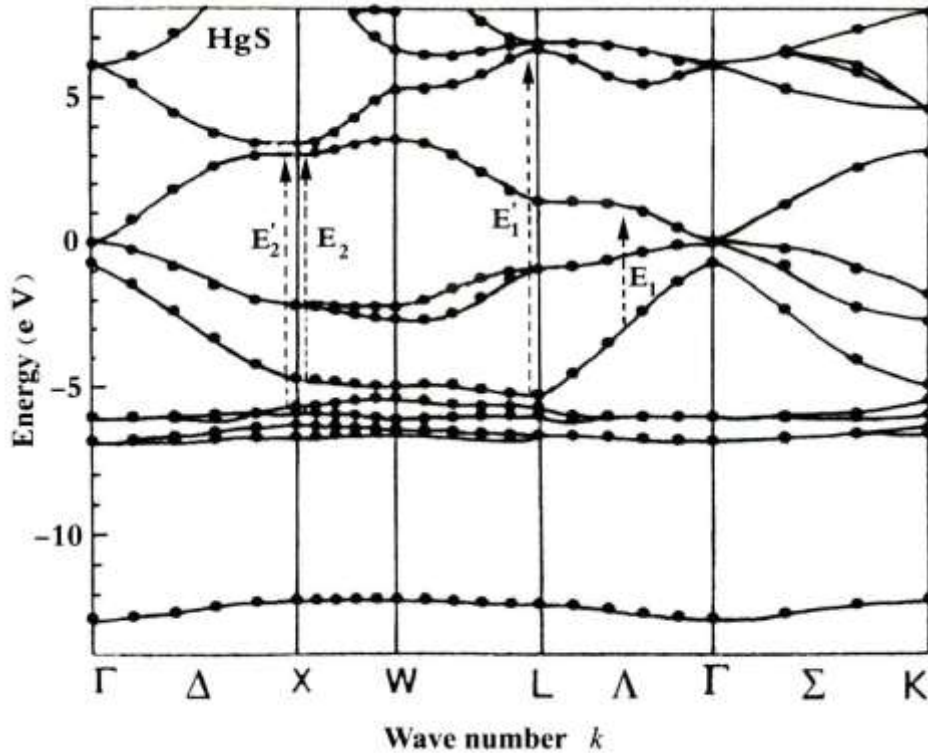


Figure 5. The optical transitions observed for  $\text{Hg}_{1-x}\text{Fe}_x\text{S}$  drawn with the calculated band structure of  $\text{HgS}$  [12]. The dashed arrows correspond to transitions that decrease with increasing Fe content, while the solid arrows correspond to transitions that increase with increasing Fe content.

A comparison of the  $\epsilon_2$  curves obtained for crystals with different Fe contents enabled us to observe changes of positions and heights of the peaks. According to Riccius and Siemsen [2] and Herman *et.al.* [3], as well as the experimental results of the reflectivity measurements [8], the structures observed in the  $\epsilon_2$  spectra arise from the optical transitions at high-symmetry points (at the critical Van Hove points) in the Brillouin zone. The maximum  $E_1$  (attributed to transitions at the  $\Lambda$  point ( $\Lambda_3^V - \Lambda_1^C$ )) at 3.46eV in the  $\square\square(h\nu)$  spectra is strongly influenced by changes in the Fe content, from 3.46eV for  $x=0.01$  to 3.22eV for  $x =0.06$  (about 0.24eV to lower energies), and changes in peak heights are much clearer. The maximum  $e_1$  (attributed to transitions at the L point ( $L_3^V - L_1^C$ )) shows also clear change of position and shifts to lower energies with increasing of  $x$ , about 0.21eV. In contrast to reflectivity spectra, which show this peak is shifting to higher energies, about 0.22eV (see Table I). For energies higher than 6eV, all the features are shifted to higher energies and partly smeared out as the amount of iron increases: the maximum  $E_2$  (attributed to transitions at the X point ( $X_5^V - X_1^C$ )) shifts from 6.72eV for  $x=0.01$  to 7.44eV for  $x=0.06$  (about 0.72eV), while the features  $E'_2$  (attributed to transitions at the X point ( $X_3^V - X_1^C$ )) from 8.20eV for  $x=0.01$  to 8.41eV for  $x =0.06$  (about 0.21eV), and  $E'_1$  (attributed to transitions at the L point ( $L_3^V - L_3^C$ )) from 9.5eV for  $x=0.01$  to 10.80eV for  $x =0.06$  (about 1.30eV). Their physical origins are similar to those ascribed to the corresponding reflectivity features (see figure 3(b) and table I).

We know that the valence band structure of the  $A^{II}B^{VI}$  crystals is constructed prevalently from the p-like states of the group VI atom, while in the other parts of the valence band a contribution of the s-like states of the group II atom hybridized with the p-like states of the group VI atom appears. The lowest conduction band is built up of the s-like electrons of the cation (group II). In mixed crystals, Fe (configuration  $3d^6 4s^2$ ) substitutes for the group II element. The two 4s electrons of Fe, together with two electrons of the group II atom, create the conduction band. Upon increasing the amount of Fe, there is a large admixture from the Fe 4s states in comparison with the s states of the group II element. Also, occupied and unoccupied Fe 3d states appear at random. Hence, it is reasonable to search for an explanation for the changes in the electronic structure in the crystals in the presence of the Fe 3d and Fe 4s states.

As for the energy gap  $E_0$ , due to  $\Gamma$  transition, it is weak to be seen in the reflectivity and  $\Gamma$  ( $h\nu$ ) spectra. In spite of that, there is a contribution of the Fe states to the  $\Gamma$  states. Dybko *et al.* [13] has been estimated the position of the Fe donor impurity to be 260meV above the bottom of the conduction band of HgS. Also, the considerable Fe3d admixture in the upper valence band has been confirmed by photoemission study reported by Kowalski *et al.* [14]. They measured resonant photoemission spectra of cubic  $Hg_{0.94}Fe_{0.06}S$  for photon energies near to the energy of intra-atomic  $Fe3p^63d^6 \rightarrow 3p^53d^7$  transition. The difference between the spectra taken at resonance and anti-resonance is presented as a measure of the energy distribution of Fe3d derived states. The results obtained show that Fe3d states contribute to the whole valence band with distinct structure appearing at the band edge. They showed three additional structures at 0.7, 2.3 and 3.9eV below the valence band maximum, in the valence band region. The feature 0.7eV was related to p-d hybridization close to  $\Gamma$ . Following Kowalski *et al.* [14], the feature about 0.7eV, occurring close to  $\Gamma$  point of the Brillouin zone agrees well with our suggestion that there exists mutual influence of the electrons in the valence band close to  $\Gamma$  with the d electrons of Fe. Hence, one can also expect that the band gap opens up. This expectation is in agreement with the results reported by Szuskiewicz *et al.* [15] for  $Hg_{1-x}Fe_xSe$ , though it has not yet been experimentally established for  $Hg_{1-x}Fe_xS$ .

It is clear from the assignment of the peaks, listed in table I, that the features sensitive to the Fe contents are ascribed to transitions at (or close to) the high-symmetry points in the Brillouin zone (BZ).

The sensitivity of the feature  $E_1$  to the presence of Fe suggests that the bands along  $\Gamma$   $\Gamma$  L direction are quite strongly influenced by the Fe-derived states that are expected to occur in both in the valence and conduction bands. This suggests that the minimum of the conduction band moves to lower energies at about 0.24eV with increasing Fe content. It may be taken as evidence for existence and influence of Fe3d empty states on conduction band.

The  $e_1$  and  $E_1'$  features represent the transitions near L point of the BZ, to the lowest and second conduction bands. These structures are sensitive to an increase of the Fe content. Also, it is clear from table I, that these transitions have the same initial state  $L_3^V$ . The  $L_3^V$  upper valence region remains roughly stationary. In contrast, the  $L_3^C$  conduction band minimum increases, owing to the large admixture cations contributing to this state (a 4s admixture Fe, as compared with 6s). The  $L_3^C$  state energy increases by about 1.30eV, and it overlaps the  $L_1^C$  state. Thus, the  $L_1^C$  conduction band moves slightly to higher energies, whereas the  $L_3^C$  state energy increases strongly one. Hence, we expect that the strong shift in

the upper conduction band region, results mainly from hybridization of the L final states with occupied or empty states of Fe ions.

The maxima  $E_2$  and  $E_2'$  revealed at 6.72eV and 8.20eV originate from the optical transitions at X point. As can be seen in table I, these structures shift strongly towards higher energies as x increases. In addition, these transitions from the valence band  $X_5^V$  and  $X_3^V$  to the  $X_1^C$  conduction band level (the first-lowest conduction band). This behaviour is like that of the L final states, i.e. hybridization of the X states with the empty Fe3d states.

### III. Summary:

In this paper we have presented results of the calculated spectra of  $\theta$ , n, k,  $\epsilon_1$ , and  $\epsilon_2$  resulting from the Kramers-Kronig analysis study of the  $\text{Hg}_{1-x}\text{Fe}_x\text{S}$  crystals (x=0.01, 0.04, 0.06) in the energy range 1.5-12eV. The energy positions of the  $\epsilon_2$  structures are consistent with previous results [2, 3, 8].

The behavior of the spectra described above can also be connected with the symmetry properties of the band structure. At points of low symmetry, Van Hove singularities, connected with the particular shape of the crystal potential, and not determined by the point group of the crystal, can be easily removed by the absence of any long-range order. On the other hand, at the high-symmetry points, the sharp bands may become somewhat broader as a result of disorder, but the high density of states (occurring due to the condition  $\nabla_k \epsilon_v = \nabla_k \epsilon_c = 0$ ) does not disappear, and strong optical transitions may still take place. Thus, we can observe that the presence of Fe ions influences the optical properties of  $\text{Hg}_{1-x}\text{Fe}_x\text{S}$  mainly by means of the disorder occurring in the lattice. No particular feature has been discerned that may be connected with the appearance of new maxima of the Fe-derived density of states

## References:

- [1]. SIEMSEN, K. J.; RICCIUS, H.D. *Phys. Stat. Solidi* 37, 1970, 445; SIEMSEN, K. J.; RICCIUS, H.D. in *Handbook on Physical Properties of Semiconductors, Volume 3: II–VI Compound Semiconductors*, (Springer US) 2004, 403-418
- [2]. RICCIUS, H. D.; SIEMSEN, K. J. in *The Physics of Semimetals and Narrow-Gap Semiconductors*, Ed. by CARTER, D. L. and BATE, R.T. (Pergamon Press, Oxford) 1971, 493.
- [3]. HERMAN, F.; KORTUM, R. L.; KUGLIN, C. D.; SHAY, J. L. *Proc. Int. Conf II-VI Semiconducting Compounds*, R.I. PROSVIDENCE, Ed. By THOMAS, D.G (W. A. Benjamin, New York) 1967, 503.
- [4]. PHILLIPS, J. C.; VAN VECHTEN, J. A. *Phys. Rev. B* 9, 1970, 2147.
- [5]. ZALLEN, R.; SLADE, M. *Solid State Commun.* 8, 1970, 1291.
- [6]. ROBERTS, G. G.; LIND, E. L.; DAVIS, E. A. *J. Phys. Chem. Solids* 30, 1969, 833.
- [7]. GUZIEWICZ, E.; KOWALSKI, B.; ORLOWSKI, B. A.; DYBKO, K.; WITKOWSKA, B.; SZUSZKIEWICZ, W. *Acta Phys. Polonica* A87, 1995, 395.
- [8]. SAREM, A. *Tishreen University Journal* Vol. 24, No. 11, 2002, 58.
- [9]. SCOULER, W. J.; WRIGHT, G. B. *Phys. Rev. B* 133, 1964, 7736.
- [10]. WOOTEN, F. *Optical Properties of Solids* (Academic, New York), 1972, 248.
- [11]. DRESSELHAUS, S.M. *Solid State Physics, Part II, Optical Properties of Solids*, 2001, 62-62.
- [12]. XIAOJIE CHEN; XINLEI HUA; JINSONG HU; LANGLOIS, J. M.; GODDARD, W. A. *Phys. Rev. B* 53, 1996, 1377.
- [13]. DYBKO, K.; SZUSZKIEWICZ, W.; WITKOWSKA, B. *defect and diffusion form*, Vol. 121-122, 1995, 41.
- [14]. KOWALSKI, J. B.; SZUSZKIEWICZ, W.; ORLOWSKI, B. A.; HE, Z.Q.; ILVER, L.; KANSKI, J.; NILSSON, P. O. *J. Electron Spectro. Related Phenom.* 85, 1997, 17.
- [15]. SZUSZKIEWICZ, W.; GUZIEWICZ, E.; KOWALSKI, J. B.; ORLOWSKI, B. A.; WITKOWSKA, B. *Mater. Sci. Forum*, 182-184, 1995, 707.